

Template-Assembled Synthetic G-Quartets (TASQs): multiTASQing Molecular Tools for Investigating DNA and RNA G-Quadruplex Biology

David Monchaud

▶ **To cite this version:**

David Monchaud. Template-Assembled Synthetic G-Quartets (TASQs): multiTASQing Molecular Tools for Investigating DNA and RNA G-Quadruplex Biology. Accounts of Chemical Research, 2023, 10.1021/acs.accounts.2c00757 . hal-03956357

HAL Id: hal-03956357
https://hal.science/hal-03956357

Submitted on 25 Jan 2023

HAL is a multi-disciplinary open access archive for the deposit and dissemination of scientific research documents, whether they are published or not. The documents may come from teaching and research institutions in France or abroad, or from public or private research centers.

L'archive ouverte pluridisciplinaire **HAL**, est destinée au dépôt et à la diffusion de documents scientifiques de niveau recherche, publiés ou non, émanant des établissements d'enseignement et de recherche français ou étrangers, des laboratoires publics ou privés.

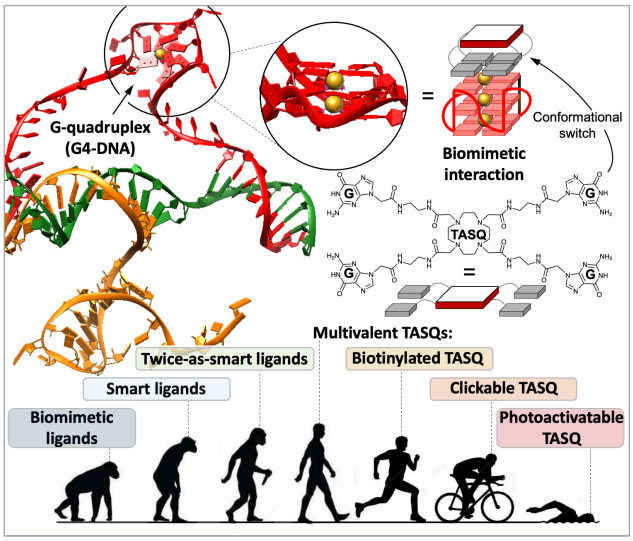
Template-assembled synthetic G-quartets (TASQs): multiTASQing molecular tools for investigating DNA and RNA G-quadruplex biology

David Monchaud

ICMUB, CNRS UMR6302, UBFC, 21078 Dijon, France

david.monchaud@cnrs.fr

Conspectus



Biomimetics is defined as a *"practice of making technological design that copies natural processes"*, with the idea that "*nature has already solved the challenges we are trying to solve*" (Cambridge Dictionary). The challenge we decided to address several years ago was the selective targeting of G-quadruplexes (G4s) by small molecules (G4-ligands). Why? Because G4s, which are four-stranded DNA and RNA structures that fold from guanine (G)-rich sequences, are suspected to play key biological roles in human cells and diseases. Selective G4-ligands can thus be used *as small-molecule modulators to gain a deep understanding of cell circuitry* where G4s are involved, thus complying with the very definition of chemical biology applied here to G4 biology (Stuart Schreiber). How? Following a biomimetic approach that hinges on the observation that G4s are stable secondary structures owing to the ability of Gs to self-associate to form G-quartets, and then of G-quartets to self-stack to form the columnar core of G4s. Therefore, using a synthetic G-quartet as a G4-ligand represents a unique example of biomimetic recognition of G4s, relying on a like-likes-like approach.

We formulated this hypothesis more than a decade ago, stepping on years of research on Gs, G4s and G4-ligands. Our approach led to the design, synthesis and used of a broad family of synthetic G-quartets, also referred to as TASQs for template-assembled synthetic G-quartets (John Sherman). This quest led us across various chemical lands (organic and supramolecular chemistry, chemical biology and genetics), along a route on which every new generation of TASQ was a milestone in the growing portfolio of ever smarter molecular tools to decipher G4 biology. As discussed in this Account, we detail how and why we successively develop the very first prototypes of *i*- biomimetic ligands, which interact with G4s according to a bioinspired, *like-likes-like* interaction between two G-quartets, one from the ligand, the other form the G4; *ii*- smart ligands, which adopts their active conformation only in the presence of their G4 targets; *iii*- twice-as-smart ligands, which act as both smart ligands and smart fluorescent probes, whose fluorescence is triggered (turned on) upon interaction with their G4 targets; and *iv*- multivalent ligands, which display additional functionalities enabling the detection, isolation and identification of G4s both *in vitro* and *in vivo*. As discussed in this Account, this quest thus led us to gather a panel of 14 molecular tools which were used to investigate the biology of G4s at a cellular level, from basic optical imaging to multi-omics studies.

Key references

- Haudecoeur, R.; Stefan, L.; Denat F.; Monchaud, D. A model of smart G-quadruplex ligand. *J. Am. Chem. Soc*., **2013**, *135*, 550.[1] *We reported on the very first prototype of a smart G-quadruplex (G4) ligand (^{PNA}DOTASQ) and demonstrated the topological switch triggered by the G4 targets that constitutes the very basis of its exquisite and uniquely active selectivity for G4s*.

- Laguerre, A.; Hukezalie, K.; Winckler, P.; Katranji, F.; Chanteloup, G.; Pirrotta, M.; Perrier-Cornet, J.-M.; Wong, J.-M.; Monchaud, D. Visualization of RNA-quadruplexes in live cells. *J. Am. Chem. Soc.,* **2015**, *137*, 8521.[2] *We reported on a 'twice-as-smart' quadruplex ligand (N-TASQ), both a smart quadruplex ligand and a smart fluorescent probe, which allowed for the very first, direct visualization of RNA quadruplexes in living human cells.*

- Yang, S. Y.; Lejault, P.; Chevrier, S.; Boidot, R.; Robertson, A. G.; Wong, J. M. Y.; Monchaud, D. Transcriptome-wide identification of transient RNA G-quadruplexes in human cells. *Nat.*

Commun. **2018**, *9*, 4730.[3] *We reported on the G4RP-seq protocol, combining G4-RNA-specific precipitation using the biotinylated BioTASQ with sequencing, which allowed for both confirming the existence of RNA quadruplexes in functional human cells and demonstrating their relevance as targets for anticancer strategies*.

- Mitteaux, J.; Lejault, P.; Wojciechowski, F.; Joubert, A.; Boudon, J.; Desbois, N.; Gros, C. P.; Hudson, R. H. E.; Boule, J.-B.; Granzhan A.; Monchaud, D. Identifying G-quadruplex-DNA–disrupting small molecules. *J. Am. Chem. Soc*., **2021**, *143*, 12567.[4] *As an application of TASQs, we reported on the first example of a small-molecule able to unfold G-quadruplexes (PhpC) in vitro, whose ability to modulate G-quadruplex landscapes in cells was established using TASQs (by optical imaging and G4RP).*

Introduction

In 2004, Jeffery T. Davis brightly summarized in his review entitled '*G-quartets 40 years later*'[5] the state of the knowledge on the G-quartet, defined as "*an hydrogen-bonded macrocycle formed by cation-templated assembly of guanosine"*. Guanosine, and more generally any guanine (G) derivative, is indeed a quite unique nucleobase: beyond its natural involvement in the double helix of DNA, in which it is associated with a cytosine, it can also create a network of different hydrogen bonds (H-bonds) *via* its two faces (Figure 1A): the Watson-Crick face[6] is embedded in three H-bonds with a cytosine, and the Hoogsteen face[7] can bind to various nucleobases including G itself to create either linear (G-ribbons) or cyclic suprastructures (G-quartet).[8]

I had the chance to meet Jeff Davis in Louisville, KY (USA) in 2007, during the first international meeting on quadruplex-DNA.[9] We notably discussed about his recently published article in which he used cross-linkable Gs to assemble a synthetic G-quadruplex (G4),[10] defined as a "*structure built from the vertical stacking of multiple G-quartets*". After the cation (K^+)-promoted formation of several contiguous G-quartets, the lipophilic G derivative 5'-(3,5-bis(allyloxy)benzoyl)-2',3'-isopropylideneguanosine **1** (Figure 1B) reacted with its neighbors *via* olefin metathesis to provide a covalently linked G4 comprising 4 stacked G-quartets (on average). We then discussed about the possibility of controlling the metathesis step not to obtain a synthetic G4 but a synthetic G-quartet: this would allow for obtaining an ideal,

bioinspired G4-ligand, fully in line with my main interest at that time (the ligand we developed with Marie-Paule Teulade-Fichou, PhenDC$_3$, was just published[11] and was precisely the topic of the poster in front of which this discussion occurred). We came to the conclusion that this approach was not controllable enough for obtaining a synthetic G-quartet, the discussion stopped there but an idea was born.

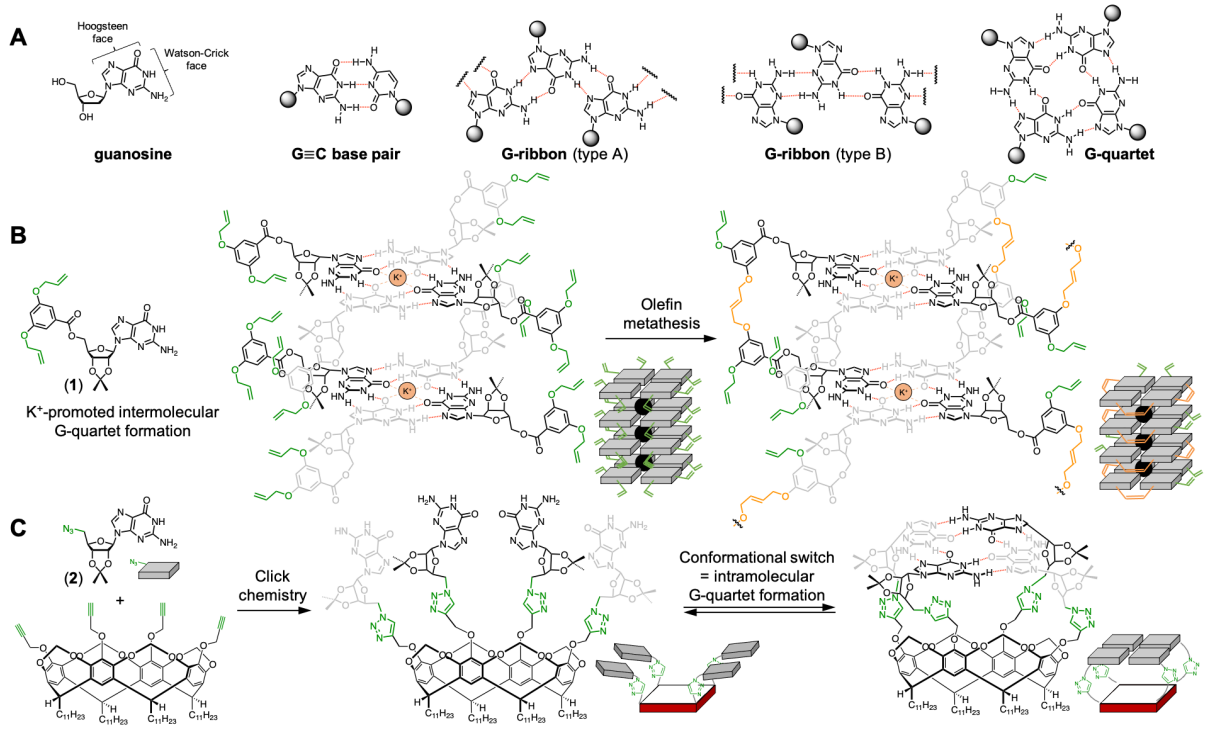


Figure 1. **A**. Chemical structure of guanosine and its possible supramolecular assemblies (GC base pair, G-ribbon and G-quartet). **B**. J. T. Davis' approach to synthesize a unimolecular, covalent G4 *via* olefin metathesis. **C**. J. C. Sherman's approach to synthesize an intramolecular G-quartet referred to as template-assembled synthetic G-quartet (TASQ) *via* click chemistry.

While challenging intermolecularly, the assembly of an intramolecular synthetic G-quartet was demonstrated to be possible one year later: John C. Sherman reported on the synthesis of a template-assembled synthetic G-quartet (TASQ),[12] in which four lipophilic guanosines 5'-azido-2',3'-O-isopropylideneguanosines **2** (Figure 1C) were clicked on a cavitand template. This approach provided a TASQ aimed at showing that the formation of an intramolecular G-quartet can occur in a cation-independent manner. This TASQ was used as a prototype, being conveniently soluble in organic media in which in-depth NMR studies were possible. We reasoned that a water-soluble template would lead to TASQs usable in biologically-relevant media, the design of the very first biomimetic G4-ligand was on its track.

From this very origin, the design of water-soluble TASQs has progressively evolved to provide ever smarter biomimetic G4-ligands that are now used as multivalent molecular tools to gain deep insights into G4 biology. This Account describes this evolution, after briefly reviewing what is known about G4s (their prevalence and functions) and why G4-ligands in general, and TASQs in particular, have been pivotal tools in this thrilling chemical biology quest.

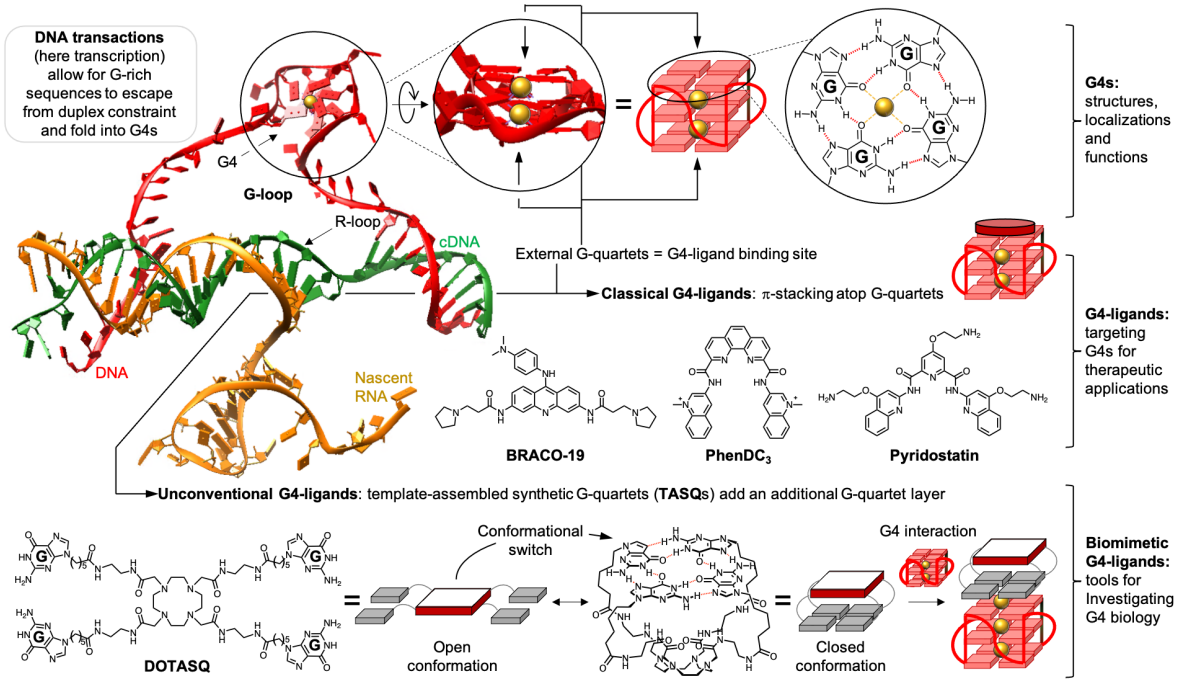


Figure 2. Schematic representation of a G-loop, which results from the cotranscriptionally formation of a R-loop (DNA:RNA hybrid, green and yellow strands) and a G4 (red strand); details about the G4 structure and the G4-ligand preferred binding site (external G-quartet); chemical structure of classical G4-ligands (BRACO-19, $PhenDC_3$ and PDS), which stack atop the accessible G-quartet of a G4, and of a biomimetic G4-ligand (DOTASQ), with a schematic representation of its conformational plurality (open and closed conformations) at the origin of its bioinspired, '*like-likes-like*' quartet/quartet interaction with a G4.

Native G-quartets, G-quadruplexes and ligands. While supramolecular chemists soon exploited the versatile H-bonding properties of Gs to create diverse nanoobjects,[13] the recognition that naturally occurring Gs might behave alike in cells has taken a long time. Indeed, the formation of a higher-order DNA structure that might have a functional relevance[14] somewhat countered the central dogma of biology, which placed the duplex-DNA at the very heart of every cellular biology process.[15] Massive chemical biology efforts were thus needed to demonstrate that nature also tamed the unique supramolecular property of Gs by providing G-containing nucleic acid sequences with the ability to fold into G4s.[16] To make this possible, G-rich DNA sequences (*e.g.*, those found at the telomeres[17] and in gene

promoter regions)[18] must be freed from their duplex constraint: this occurs when DNA is at work, *i.e*., when being replicated or transcribed (see the schematic representation of a G-loop[19] formed during the transcription of a G-rich region in Figure 2) or being repaired. This makes G4 formation not only tightly patrolled by the protein machinery in charge of DNA transactions but also transient in nature, explaining why their detection in fixed[20] then living cells was challenging.[21]

DNA transactions thus represent a unique window of opportunity for G4s to fold, which is also recognized as vulnerable events that could jeopardize genomic stability.[22] This underpins the strategy based on the use of G4-targeting agents (or G4-ligands)[23] as therapeutic agents: by stabilizing transiently folded G4s that arise during DNA transactions, G4-ligands can indeed prevent these cellular events from being properly performed. G4s can thus stall–or even trigger the collapse of–the enzymatic machinery in charge of these transactions, which is recognized as a situation of crisis, dealt with as a DNA damage, and consequently coped with by the DNA damage response (DDR) machinery. Most cancer cells being DDR-impaired,[24] they are thus more sensitive to G4-mediated DNA damage; G4-ligands can therefore inflict severe DNA damage to cancer cells, which is at the very basis of their use as antiproliferative agents.[25]

Classical G4-ligands such as BRACO-19,[26] $PhenDC_3$[11] and pyridostatin (PDS),[27] are flat aromatic molecules ideally suited to interact with G4s by stacking atop its accessible, external G-quartet (Figure 2). Their small size and moderate charge allow them to enter cells rather readily to reach their G4 targets, where they trigger their G4-mediated cellular effects.[28] However, given that they are built on DNA-intercalator motifs (pyridine, quinoline, phenanthroline and acridine), off-target effects cannot be ruled out, even if an exquisite G4-selectivity has been achieved for some of them (*e.g.,* $PhenDC_3$, *vide infra*). This is where water-soluble TASQs come into play: owing to an intrinsic structural dynamism, TASQs exist under two conformations, an 'open' one in which the Gs are independent from each other, and a 'closed' one in which the intramolecular G-quartet is folded (see the schematic representation of DOTASQ (*vide infra*), Figure 2). TASQs thus adopt their closed, G4-*affinis* conformation only in the presence of G4s, which makes them uniquely actively selective for their G4 targets. This good selectivity, driven by a bioinspired, *like-likes-like* interaction between two G-quartets (one native from the G4, one synthetic from the TASQ), makes these ligands ideal molecular tools to investigate G4

biology. As further discussed hereafter, we spent the last decade developing different water-soluble TASQs (Figure 3) to make them evolve from biomimetic G4-ligands to multivalent molecular tools. Our goal was not to use these compounds as therapeutic agents but to design, synthesize and use ever smarter TASQ tools aimed at being used in optical imaging and large-scale, multi-omics studies in the aim of portraying G4 biology as accurately as possible.

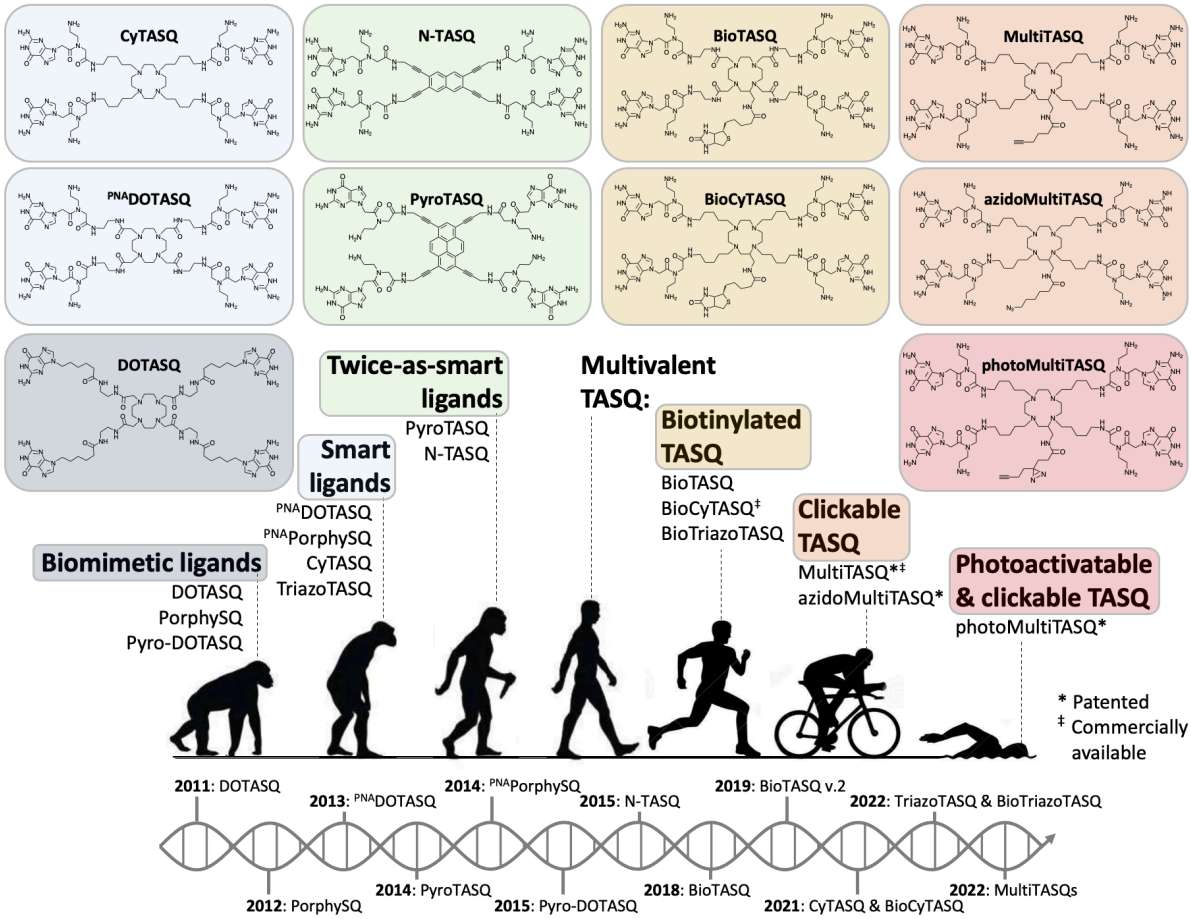


Figure 3. Evolution of water-soluble TASQs used as G4-ligands, from biomimetic to multivalent TASQs (for patented and commercially available TASQs, see[29]).

Biomimetic & smart G4-ligands. The very first prototype of water-soluble TASQ used as a biomimetic ligand was the DOTA-templated synthetic G-quartet, or **DOTASQ**,[30] comprising four Gs connected to a central DOTA (Figure 4A). This TASQ was published concomitantly (in 2011) with another water-soluble TASQ built on a macrocyclic peptide as regioselectively addressable functionalized template (RAFT).[31] This 'RAFT-G4'[32] was not used as a G4 ligand but rather to demonstrate by nuclear magnetic resonance (NMR) that a synthetic G-quartet

can fold in water. Sherman also reported on a water-soluble version of his cavitand-based TASQs[33] two years later (in 2013) but again, this TASQ was not used as a G4 ligand but rather as a platform to study the interaction between an isolated G-quartet (TASQ) and a G4 ligand (*e.g.*, BRACO-19). **DOTASQ** was thus the very TASQ to be investigated as a biomimetic G4 ligand but the first results were disappointing: no G4-stabilization was obtained when subjected to FRET-melting evaluations (Figure 4B) performed with a doubly labelled G4-forming oligonucleotide mimicking the human telomeric sequence (F21T).[34] We attributed this lack of interaction to a limited solubility in water (the poorly soluble G units, alkyl arms and amide connectors strongly counterbalanced the water-solubility of DOTA) and a high flexibility of both G arms and template (which might preclude the formation of a stable intramolecular G-quartet).

To tackle these issues, we exploited the property for which DOTA is thoroughly used, *i.e.*, the metal chelation. We selected terbium, with an eye towards possibly benefiting from its luminescent properties (*vide infra*) if the presence of a metal within the DOTA cycle proved to be an effective way to tame DOTASQ structural flexibility. The coordination of a terbium ion within the DOTA cavity resulted in the tricationic complex [**Tb.DOTASQ**]$^{3+}$ (Figure 4A) that was consequently more geometrically constrained, water-soluble and poised to interact electrostatically with DNA. Satisfyingly, this complex stabilized G4s, although modestly, as it increased the mid-transition temperature ($\Delta T_{1/2}$) of the G4 by *ca*. 10°C, which is routinely used as a proxy for G4 affinity (of note: $PhenDC_3$ imparts a >30°C-stabilization in similar conditions). This fair apparent affinity, which was confirmed with other G4-forming sequences mimicking the promoter regions of MYC and KIT genes, provided the proof of concept we were eagerly awaiting. These experiments were also performed in presence of an excess of unlabelled, 26-nt long duplex-DNA competitor (ds26): the G4-stabilization imparted by the ligand was marginally affected only (-15% in the presence of 50 molar equivalents (mol. equiv.) of ds26, *versus* -10% for $PhenDC_3$ in similar conditions),[11] demonstrating a very good G4-selectivity of [**Tb.DOTASQ**]$^{3+}$ over duplex-DNA, which confirmed the relevance of our bioinspired design.

However, this complex turned out to be chemically unstable, likely because the DOTA was not the most suited chelator for terbium. We nevertheless tried to exploit its luminescence properties by inserting a sensitizing antenna on the DOTA scaffold (*cf*. [**Tb.Pyro-DOTASQ**]$^{3+}$,

Figure 4A),[35] but with a moderate success only. We thus envisioned two strategies to address these issues. First, we increased the stability of the intramolecular G-quartet by using a template known to strongly interact with G-quartets. To this end, we used a porphyrin template, as this scaffold is found in one of the most used G4-ligand TMPyP4 (which should nevertheless be avoided because of its indiscriminate interaction with DNA, whatever its structure).[36] The resulting porphyrin-templated synthetic G-quartet, or **PorphySQ**,[37] showed a very weak G4-interaction (although with an excellent G4-selectivity). These results were further compounded by a very poor water-solubility. We thus replaced the neutral G units by protonable Gs. Indeed, the Boc-^{PNA}G-OH monomer is another G unit that harbors an ethylamine sidechain, readily protonated at pH 7.2, which makes it both water-soluble and prone to good electrostatic interactions with DNA. We thus assembled four ^{PNA}Gs around either a DOTA or a porphyrin template: the resulting TASQ, **^{PNA}DOTASQ**[1] and **^{PNA}PorphySQ**[38] (Figure 4A) thus displayed a tetracationic synthetic G-quartet (once folded) suited to strongly interact with a tetraanionic native G-quartet. **^{PNA}PorphySQ** displayed better performance than **PorphySQ** ($\Delta T_{1/2}$ *ca*. 7 °C for both telomeric and KIT G4s); however, it suffered from a modest water-solubility and a self-immolating nature (likely *via* internal porphyrin-mediated photooxidation of G units). By contrast, **^{PNA}DOTASQ** provided excellent results: its affinity for G4s was good ($\Delta T_{1/2}$ > 12°C for telomeric, MYC and KIT G4s, Figure 4B), its selectivity excellent, (though slightly lower than the parent compound **DOTASQ**, -26% in the presence of 50 mol. equiv. of ds26) and the chelation of terbium was no longer required.

We next wondered whether **^{PNA}DOTASQ** interacts with both DNA and RNA G4s: competitive FRET-melting experiments showed a good affinity for RNA G4s ($\Delta T_{1/2}$ > 10°C for the sequences found in the telomeric transcript TERRA and the untranslated regions (5'-UTR) of TRF2 and VEGF mRNA), which was only marginally affected (>-13%) in the presence of 50 mol. equiv. of an unlabeled, highly stable DNA G4 competitor (TG5T).[39] These results did not indicate a selectivity for G4-RNA over G4-DNA but a preferential interaction with the former, likely due to a better G-quartet accessibility. Globally speaking, ^{PNA}DOTASQ was considered as a pan-G4 interacting agent as it did interact with G-quartet whatever the G4 to which it belongs. These G4-interacting properties were satisfying enough to go further than simple G4-affinity measurement and we used it to gain insights into the way it interacts with G4s: the 1:1 stoichiometry of the **^{PNA}DOTASQ**/G4 association was shown by electrospray ionization mass

spectrometry (ESI-MS),[40] and no 2:1 TASQ/G4 complex was detected. The demonstration that this TASQ adopts its closed conformation upon interaction with G4s was provided by NMR (Figure 4C).[41] As duplex-DNA failed in promoting such an internal conformational switch, these results showed that only G4s can drive **^{PNA}DOTASQ** into its closed, G4-affinic conformation, making it the very first prototype of a smart G4-ligand.

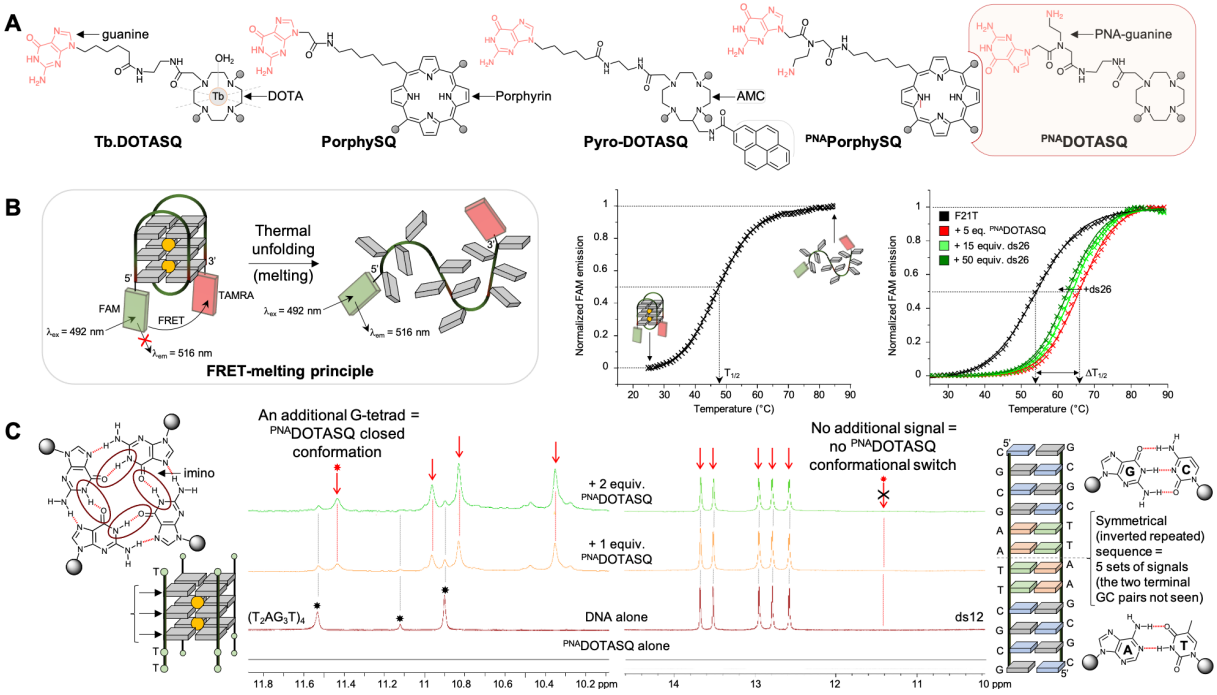


Figure 4. **A**. Chemical structure of biomimetic (Tb.DOTASQ, PorphySQ and Pyro-DOTASQ) and smart ligands (^{PNA}PorphySQ and ^{PNA}DOTASQ). **B**. Schematic representation of the FRET-melting assay (left) and results collected with a doubly labelled G4 in absence (center, whose stability is quantified by the mid-transition temperature $T_{1/2}$) or presence of a ligand (right), here ^{PNA}DOTASQ (with the $\Delta T_{1/2}$ value used as a proxy for G4 apparent affinity), without or with an excess of the duplex competitor ds26. **C**. NMR results collected with a G4 (left) or a duplex (right) upon addition of increasing concentrations of ^{PNA}DOTASQ, which demonstrate the conformational switch of the ligand triggered by its G4 target.

We next aimed at endowing TASQs with additional skills in order to use them as molecular tools, notably to demonstrate the existence of G4s in human cells. We first focused on optical imaging and devised new TASQs implementable as smart G4 fluorescence probes.

Twice-as-smart G4-ligands. The TASQ design was further modified to convert them into valuable fluorescent probes. Specifically, we sought for a dye whose fluorescence properties could be modulated as a function of the TASQ conformation: a different response depending on the TASQ's open or closed status would lead to a turn-on fluorescence probe that would represent the fine art of G4 detection.[42] This template should thus be fluorescent and sensitive

to the presence of Gs in its close proximity, have a pseudo-C_4 symmetry and allow for an easy introduction of four G arms.

We selected a pyrene template as its fluorescence is known to be hypersensitive to proximal G quenchers.[43] We used unsaturated connectors (alkyne linkers) to extend the aromaticity of the template in order to displace its excitation wavelength (λ_{ex}) towards an optical window suited to optical cell imaging. This novel TASQ, named pyrene-templated synthetic G-quartet, or **PyroTASQ**,[44] was readily assembled through a quadruple Heck-Cassar-Sonogashira coupling (Figure 5A).[45] Its affinity for G4s was good ($\Delta T_{1/2}$ > 13°C for telomeric, MYC and KIT G4s), its selectivity excellent (-16% in the presence of 50 mol. equiv. of ds26) and its ability to interact with G4s adopting its closed conformation demonstrated by NMR. Its photophysical properties were enticing: its fluorescence (λ_{ex} = 420 nm; λ_{em} = 440 nm) was satisfyingly quenched when free in solution, strongly enhanced (up to 90-fold) upon addition of G4s and insensitive to the presence of a large excess of genomic DNA once turned-on by G4s.

The mechanism behind the spectroscopic properties of **PyroTASQ** was further investigated. Free Gs (open conformation) were known to quench the pyrene fluorescence by photoinduced electron transfer (PET). We assumed that their self-association into the G-quartet (closed conformation) would trigger a redistribution of their electron density over the whole macrocycle *via* either resonance-assisted H-bonding (RAHB)[46] or charge separation,[47] or both. This, combined with the π-stacking interaction with the accessible G-quartet of a G4, would contribute to decrease the electron density of each G and thus, alleviate the PET-mediated quench of the pyrene fluorescence. This explanation provided a satisfying rationale for the turn-on properties of **PyroTASQ** but was too simple. A combination of geometrical optimizations and density functional theory (DFT) calculations (Figure 5B)[48] showed that the open conformation actually corresponds to a conformation in which at least one G is stacked atop the template, and the highest occupied molecular orbital (HOMO) is localized on the whole TASQ structure. Upon irradiation, the energy is dissipated in a non-radiative manner by the freely vibrating G and an internal energy transfer from the pyrene to the G allows to channel the energy accumulated by the template to Gs for dissipation. In the closed conformation, the HOMO is exclusively localized on the template, precluding charge transfer with Gs, which are anyway embedded in the G-quartet and thus, no longer free to dissipate

this energy through vibrational motion. The energy accumulated by the template is thus dissipated through fluorescence emission. **PyroTASQ** was thus the first prototype of a twice-as-smart G4-ligand, being both a smart G4-ligand and a smart fluorescent probe.

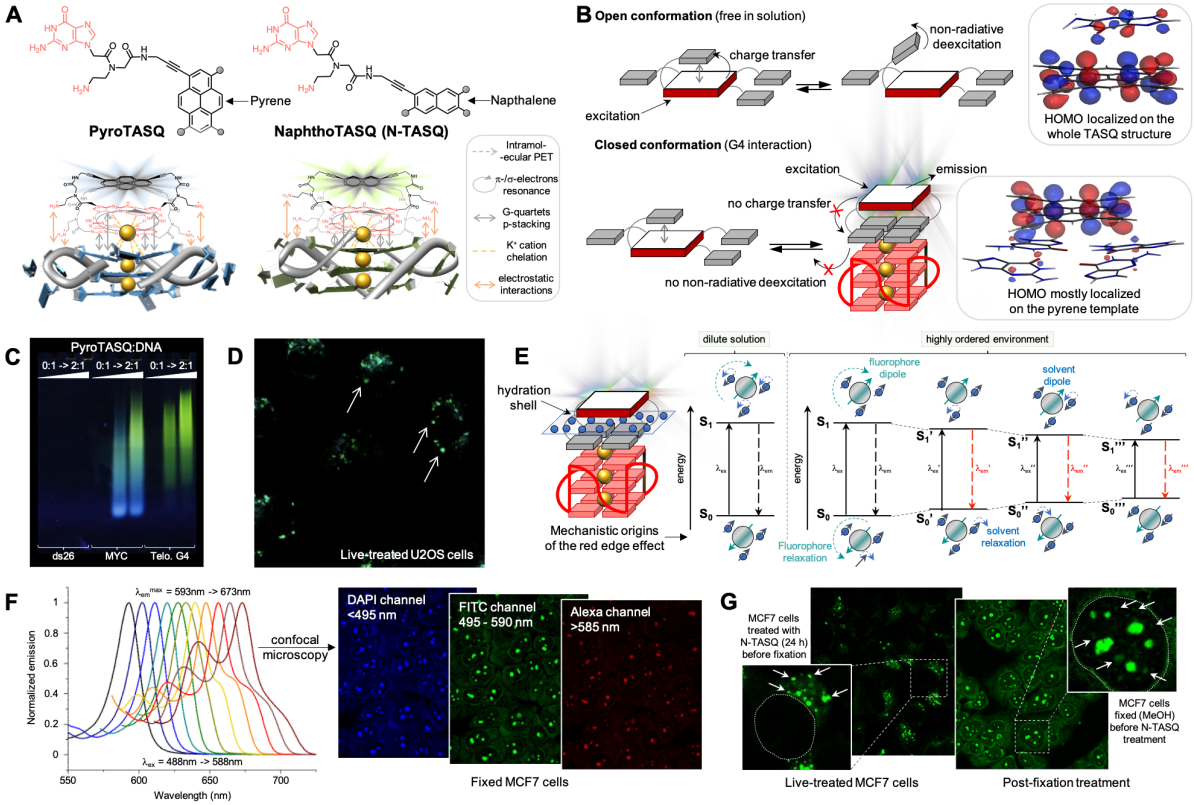


Figure 5. **A**. Chemical structure of the twice-as-smart G4 ligands PyroTASQ and NaphthoTASQ (N-TASQ) and schematic representation of their interaction with G4s, which triggers their fluorescence (turn-on probe). **B**. Schematic representation of the mechanism behind the turn-on fluorescence properties of TASQs (molecular orbital analyses performed at BLYP-D3/TZP level of DFT gas phase calculations). **C**. Fluorescence analysis of a polyacrylamide gel performed with DNA (telomeric and MYC G4s or the duplex ds26) and increasing amounts of PyroTASQ. **D**. Live-cell imaging of U2OS cells treated with N-TASQ (5 μM for 48 h) collected with a two-photon microscope (λ_{ex} = 720 nm). **E**. Simplified Jablonski diagram depicting the ground (S_0) and excited states (S_1) of a TASQ in dilute solution (left) or ordered environment (right) where the solvent relaxation is slowed down, which give rise to the red edge effect (a continuous model of solvent relaxation with intermediate ground (S_0', S_0", etc.) and excited states (S_1', S_1", etc.) leading to red-shifted excitation (λ_{em}', λ_{em}", etc.) and emission (λ_{ex}', λ_{ex}", etc.) wavelengths). **F**. Dependence of the emission maxima (λ_{ex}^{max}) on the excitation wavelength (λ_{ex}) (left), typical of the red edge effect, which was confirmed by confocal microscopy (right) with images of MCF7 cells collected through the blue, green and red channels. **G**. Use of N-TASQ in either live cells (left) or fixed cells (right) which allow for a direct visualization of either RNA (left) or DNA (right) G4 *foci*.

These properties were used to detect G4s *in vitro*: polyacrylamide gel electrophoresis (PAGE, Figure 5C) was performed with both telomeric and MYC G4s along with a duplex-DNA as control. **PyroTASQ** provided a specific visualization of G4s using a classical gel imaging system. The fluorescence response was surprisingly smeared and two-color, being indigo for the nicely

defined bands and green for the higher molecular weight smear. We attributed these observations to a clean **PyroTASQ**/G4 interaction (indigo band) and a higher-order **PyroTASQ**/G4 complex, likely driven by the well-known tendency of pyrene to self-associate to form excimer (green smear). This tendency was confirmed during preliminary cell-based investigations, in which aggregates were found to accumulate around the cells, making the resulting images uninterpretable. A modification of the TASQ chemical scaffold was thus required, sufficient to prevent self-aggregation but not too much to keep the finely tuned G4-interacting and photophysical properties of **PyroTASQ**.

Our options were limited. Hinging on a recent report describing the straightforward synthesis of the naphthalene precursor 3,6-dibromo-2,7-bis(trifluoromethanesulfonyloxy)-naphthalene[49] suited to be engaged in a quadruple Heck-Cassar-Sonogashira coupling, we synthesized a new probe that we named naphthalene-templated synthetic G-quartet, or **NaphthoTASQ** (**N-TASQ** for short, Figure 5A).[2] We hoped that halving the aromatic surface would decrease self-association while maintaining the peculiar turn-on properties of the reference compound **PyroTASQ**. The affinity of **N-TASQ** for G4s was good ($\Delta T_{1/2}$ > 12°C for telomeric, MYC and KIT G4s) and its selectivity excellent (-11% in the presence of 50 mol. equiv. of ds26). The connection of four alkyne linkers weakly displaced the excitation wavelength (to 320 nm), leading us to exploit an indirect sensitization mode, based on an energy transfer from the G4 to the bound ligand. This energy transfer, known to be particularly efficient within G4s as mediated by cations,[50] was fully suited to the bioinspired TASQ/G4 interaction as it implies the presence of a cation in between the synthetic and native G-quartets. In doing so, we provided an interesting DNA structure-specific sensitization of **N-TASQ**, as only the addition of G4s lighted its fluorescence up (*ca*. 20-fold with MYC G4). Satisfyingly, this molecule did not aggregate and was both bioavailable (readily entering cells without permeabilization) and non-toxic (IC_{50} >100 μM after 72 h-treatment).

To circumvent the low absorbance maxima of **N-TASQ**, poorly convenient for optical imaging (leading to an elevated cell autofluorescence background), the first series of optical images using **N-TASQ** were collected with a two-photon microscope adjusted at λ_{ex} = 720 nm. Thanks to its intrinsic cell-permeability, **N-TASQ** was usable in living cells: MCF7 and osteosarcoma (U2OS) cells were live-incubated with **N-TASQ**, prior to be imaged without further

manipulations (no fixation, permeabilization, mounting steps). The collected images, which confirmed the perinuclear accumulation of RNA G4/**N-TASQ** complexes, represented the first visualization of G4s in living cells (Figure 5D). We next used **N-TASQ** on fixed and permeabilized breast cancer cells (MCF7); surprisingly (further discussed below), high-quality images were collected using a confocal microscope through the different emission filters (blue, <495 nm; green, 495 - 590 nm; and red channels, >590 nm). The actual nature of the observed *foci* was confirmed *via* by different treatments (DNase, RNAse) and colocalization with the G4-specific BG4 antibody.[51] The quality of the **N-TASQ** labelling was found to be strongly dependent on the fixation method (MeOH should be privileged); in these conditions, **N-TASQ** labelled preferentially RNA G4s (in both cytoplasmic and nucleolar sites), likely due to the higher accessibility of these targets.

These good results nevertheless raised two questions: why was a sensitization of **N-TASQ** at 720 nm efficient (it is more than double its maximal λ_{ex}) using a two-photon microscope? And why was the fluorescence observable through the blue/red/green channels using a confocal microscope? Deep spectroscopic investigations revealed that **N-TASQ** did not behave as a classical fluorescence dye: rather counterintuitively, this molecule can be sensitized at wavelengths at which it does not absorb light. This behavior, known as the red-edge effect (REE), is studied for more than 50 years notably in polymer science[52] but rarely, if ever, reported in optical cell imaging investigations. REE was timely described for a series of PNA oligomers during the course of our investigations,[53] which provided a rationale for the peculiar behavior of **N-TASQ**. Briefly, when two aromatic partners (here a G-quartet and a naphthalene template) strongly interact with each other, the water molecules trapped in between them (belonging to their hydration shell) are dissociated from bulk water. Their motion is restricted and their dielectric relaxation participates to the deexcitation of the probe: therefore, the relaxation of each water molecule provides a virtual excited state of lower energy (Figure 5E), which can be thus excited with photons of lower energy, that is, of higher wavelengths (*i.e.*, on the red edge of the absorption spectrum of the dye). This effect, possible only in media with very slow dynamics (here, in fixed cells), made the sensitization of **N-TASQ** possible at wavelengths >320 nm.

We used this properties to show that high-quality images could be collected using a classical confocal microscope, with lasers adjusted at 408, 488 and 555 nm (Figure 5F). On this basis, we devised an experimental setup to use **N-TASQ** to label either RNA G4s (live-cell **N-TASQ** incubation before fixation and imaging) or DNA G4s (cell fixation before N-TASQ incubation and imaging) (Figure 5G).[54] We also devised a quantitative use of **N-TASQ** fluorescence to assess the modulation of the G4 landscape in cancer cells (*e.g.*, HeLa) upon incubation with G4-interacting compounds, *e.g.*, the G4-stabilizer BRACO-19 was found to increase it,[55] or the G4-destabilizer PhpC[4] to decrease it (*unpublished*). **N-TASQ** was also found to be compatible with live-cell imaging systems which enables to characterize real-time at which pace it enters cells (*ca*. 12 h) and its residence time in cells (*ca*. 100 h).[55] The use of **N-TASQ** was extended to other cancer cells, notably to uncover the origin of their replicative immortality (telomerase-dependent ($TERT^+$) *vs*. telomerase-independent (ALT^+) mechanisms).[56] **N-TASQ** was also used for the detection and quantification of G4 landscapes in a series of nervous cells including neurons,[57] astrocytes[58] and microglia[59] (without or with treatment with PDS). These different applications clearly highlighted the versatility of this probe, being usable in either fixed or live cells, with different imaging apparatus, in different cell types. To go a step further, we needed to devise new molecular tools in order to identify the nucleic acid sequences (and eventually the associated proteins) the TASQs interact with in cells.

Multivalent G4-ligands. The chemistry of polycyclic aromatic hydrocarbons (PAHs, such as pyrene or naphthalene) being rather challenging,[60] we did not try to synthesize PAH derivatives that would have allowed for endowing the corresponding TASQ (**PyroTASQ**, **N-TASQ**) with additional functionalities. Our experience with **Pyro-DOTASQ** (*vide supra*) convinced us about the convenient use a the DOTA derivative named AMC (aminomethylcyclen, Figure 4A) to introduce new functionalities. We thus used the aminomethyl appendage of AMC to introduce various functional moieties on the **^{PNA}DOTASQ** scaffold. The first one was a biotin: the corresponding biotinylated TASQ, named **BioTASQ** (Figure 6A),[3] was intended to be used as a molecular bait for fishing G4-forming sequences thanks to the well-established affinity precipitation using streptavidin-coated beads.[61] Unexpectedly, the introduction of a biotin handle almost abolished the G4-affinity of the resulting TASQ, as only very weak stabilizations ($\Delta T_{1/2}$ < 2°C) were obtained during FRET-melting investigations. We ascribed this lack of affinity to an internal poisoning of one of the

G arm by H-bonding with biotin (Figure 6B). To discard simple steric reasons, we synthesized a derivative with a polyethylene glycol (PEG) linker in between the AMC template and the biotin: the resulting **BioTASQ v.2** displayed an even worse G4-stabilization,[62] confirming that the ability of biotin to create intramolecular H-bonds was indeed responsible for the loss of G4 interaction.

To tackle this, we pre-mixed **BioTASQ**s and streptavidin-coated magnetic beads, in order to hijack biotin from internal poisoning, and used this assembly to isolate G4s from solution. This was validated using fluorescently labelled G4-forming sequences (FAM-G4s) *in vitro*, along with a FAM-duplex as control. The capture efficiency of TASQs was quantified by measuring the fluorescence resulting from the dissociation of the FAM-G4/TASQ/bead complex (thermal treatment). Both **BioTASQ**s pulled down RNA G4s (11- to 44-fold fluorescence enhancement, normalized to TASQ-less control) more readily than DNA G4s (2- to 26-fold enhancement). This efficiency was slightly altered (-25%) in the presence on an excess of duplex-DNA, which was further confirmed by the lack of FAM-duplex capture (0.7-fold enhancement). This opened the way towards cell-based investigations: the ability of **BioTASQ**s to fish G4s out from cell lysates was first validated by a RT-qPCR analysis targeting well-established RNA G4-forming sequences.[63] We selected RNA targets and developed the corresponding protocol G4RP (G4-RNA precipitation, Figures 6C and D) to disentangle a paradoxical situation resulting from two conflicting reports: the rG4-seq[64] method concluded that RNA G4s were pervasive structures in the human transcriptome, while a combination of DMS-seq and RT-stop profiling[65] concluded that RNA G4s were mostly unfolded *in vivo*. We hypothesized that the formation of G4s might be transient only in cells; we thus devised the G4RP protocol introducing a fixation step to capture transiently folded G4s *in vivo* prior to cell lysis and **BioTASQ**-mediated G4-precipitation. This approach was validated by RT-qPCR against a series of well-known G4-prone transcripts including the sequence found in the 5'-UTR of NRAS and VEGF mRNAs.[3, 62] Both **BioTASQ**s efficiently pulled down RNA G4s from cell lysates (16- to 59-fold enhancement, normalized to biotin control), with a slightly better performance of **BioTASQ v.2**. We artificially forced G4-folding in cells live-incubating them with BRACO-19: this treatment increased the overall efficiency of the capture, more markedly with **BioTASQ** (up to 9-fold enrichment, normalized to untreated control) than **BioTASQ v.2** (4-fold enrichment only). These results confirmed the ability of G4-ligands to modulate G4 landscapes

in cells, in line with **N-TASQ** results described above. We next performed a transcriptome-wide analysis (G4RP-seq, Figure 6E)[3] of the same cancer cells, without or with cell incubation with BRACO-19: the results obtained first confirmed the prevalence of RNA G4s *in vivo*, with >6,000 G4-containing transcripts isolated. They also uncovered the prevalence of G4s in long non-coding RNAs (lncRNAs). And very importantly, they helped redefine both the targets and the cellular modes of action of G4-ligands: our results showed that cells evolved a mechanism (likely helicases)[66-67] to avoid G4-formation in lncRNAs that is counteracted by G4-ligands, which thus affect their functions by stabilizing a folding that is not compatible with their regular cellular activity.

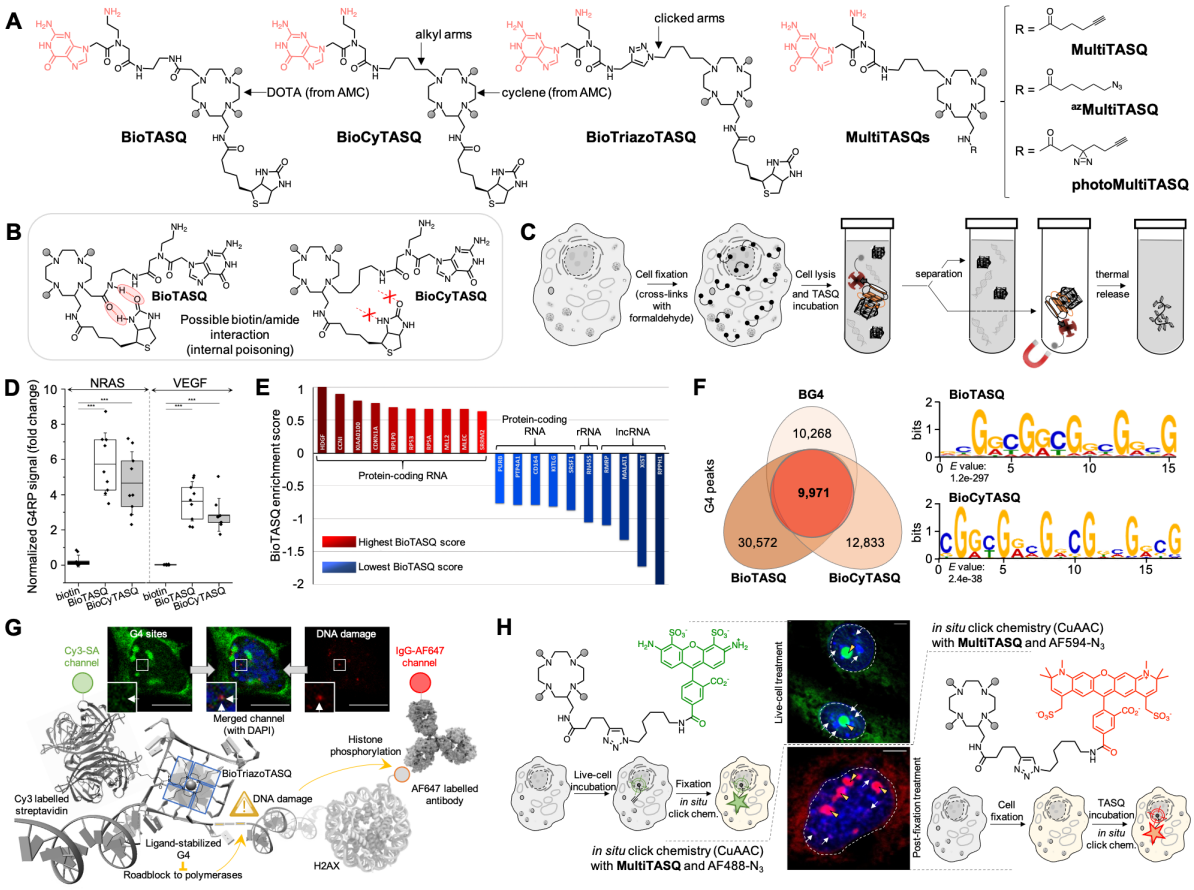


Figure 6. **A**. Chemical structure of the multivalent TASQs including the biotinylated BioTASQ, BioCyTASQ and BioTriazoTASQ and the MultiTASQs (MultiTASQ, azidoMultiTASQ ([az]MultiTASQ) and photoMultiTASQ). **B**. Schematic representation of the possible internal structural poisoning of BioTASQ. **C**-**E**. Schematic representation of the G4RP (G4-RNA precipitation) protocol (**C**) and examples of results obtained by RT-qPCR (**D**) or sequencing (**E**). **F**. Number of G4 peaks obtained by the G4DP-seq protocol (G4-DNA precipitation and sequencing) in the rice genome using BioTASQ or BioCyTASQ in comparison with that of BG4-ChIP-seq in similar conditions (using the antibody BG4); left: example of motifs enriched by the two TASQs. **G**,**H**. Schematic representation and results of pre-targeted G4 imaging (**G**) using BioTriazoTASQ (to colocalize G4 and DNA damage sites) and *in situ* click imaging (**H**) using MultiTASQ (being used as a live-cell or post-fixation agent).

We then wanted to address the overall low G4-affinity of biotinylated TASQs. We thus revisited their synthetic schemes to circumvent the biotin internal poisoning issue and make their access more straightforward. We changed the nature of the G arms, removing one amide connector to alleviate H-bonding with biotin. In doing so, the central template was not a DOTA anymore but a cyclene, which made the resulting molecule cyclene-templated synthetic G-quartets, or **CyTASQ**s. We assessed the validity of this approach with the naked **CyTASQ** (*i.e.*, without biotin handle) to verify that using such an alkyl arm did not modify the overall G4-interacting properties of the parent ^{PNA}**DOTASQ** compound. **CyTASQ** stabilized G4s modestly ($\Delta T_{1/2}$ = 5 and 9 °C for telomeric and MYC G4s, respectively), lower than ^{PNA}**DOTASQ** ($\Delta T_{1/2}$ > 12°C),[68] but its G4-selectivity was excellent (-8% in the presence of 50 mol. equiv. of ds26), better than ^{PNA}**DOTASQ**. We next synthesized the biotinylated **CyTASQ**, or **BioCyTASQ** (Figure 6A), and evaluated its G4-interacting properties: quite satisfyingly, its G4-affinity was unaffected by the presence of the biotin handle ($\Delta T_{1/2}$ = 5 and 10 °C for telomeric and MYC G4s, respectively) and its selectivity even better (-2% in the presence of 50 mol. equiv. of ds26), making **BioCyTASQ** a far better G4-ligand than **BioTASQ** ($\Delta T_{1/2}$ < 2°C). Its affinity was also assessed by a fluorescence quenching assay (FQA)[69] that confirmed its good G4 affinity (Cy5-MYC, $^{app}K_D$ *ca*. 1 μM; of note, no 2:1 TASQ:G4 complex was detected, thus confirming aforementioned ESI-MS results), while being 1 order of magnitude lower than $PhenDC_3$ ($^{app}K_D$ *ca*. 0.1 μM). We next confirmed that **BioCyTASQ** did capture RNA G4s as did **BioTASQ** by performing a G4RP-RT-qPCR analysis of MCF7 cell lysate against NRAS and VEGF (Figure 6D).

With these results in hand, we wanted to meet another challenge: using biotinylated TASQs to capture and identify DNA G4s *in vivo*. Inspired by the G4RP-seq protocol, we developed the G4DP-seq (G4-DNA precipitation and sequencing) using a model genome, the rice genome. This model benefitted from a straightforward access to high-quality genomic DNA, ideally suited to perform comparative studies in which G4s were captured by either **BioTASQ**, **BioCyTASQ** or BG4. This approach thus represented an unprecedented comparison of the efficiency of affinity-based G4 purification protocols, *i.e.*, chemoprecipitation (G4DP-seq)[70] *vs*. immunoprecipitation (BG4-IP-seq),[71] in line with our comparison of chemodetection (N-TASQ) *vs*. immunodetection (BG4) of G4s.[56] The collected results (Figure 6E) confirmed that small molecules competed with antibodies for the isolation of G4s: while BG4-IP-seq identified *ca*. 30,000 G4 peaks, G4DP-seq identified *ca*. 70,000 G4s with **BioTASQ** and 50,000 G4s with

BioCyTASQ.[70] These numbers were not commensurate with that of G4s detected in human cells (>500,000 G4 peaks),[72] likely originating in a more suppressive effect on higher-order DNA structure formation in plant genomes, as a similar trend was observed with C-quadruplexes (or i-motifs),[73] *ca*. 25,000 peaks in plants[74] *vs.* >600,000 peaks in human cells.[75] G4DP-seq and BG4-IP-seq captured G4s in *in vitro* conditions, that is, with G4-forming sequences from fragmented DNA properly folded prior to be precipitated by affinity capture. A fine analysis of the difference between **BioTASQ** and **BioCyTASQ** revealed a majority of common G4 peaks (*ca*. 82%) but a longer average length of G4 peaks for **BioCyTASQ**. We then compared the efficiency of TASQs in *in vitro vs*. *in vivo* conditions, where naturally folded G4s were cross-linked live prior to cell lysis, chromatin fragmentation and affinity capture steps. A similar amount of G4 peaks was detected (*ca*. 60,000 peaks), with >70% common peaks with *in vitro* conditions, highlighting the suitability of TASQ probes to the two approaches.

We then modified again the synthetic access to biotinylated TASQs to assemble the G arms by click chemistry, a guarantee of efficiency and rapidity. The resulting TASQs, which harbored a triazole linker within their G arms, were consequently termed **TriazoTASQ** and **BioTriazoTASQ** (Figure 6A).[76] Both compounds displayed high affinity and selectivity for G4s: while **BioTriazoTASQ** has not yet been used for G4RP/G4DP investigations, it was used in a pre-targeted G4 imaging protocol to detect G4s in human cells thanks to the labelling of **BioTriazoTASQ** once in its cellular binding sites by a fluorescently labelled streptavidin (Figure 6G). This strategy was validated using **BioTASQ** and **BioCyTASQ**, the live-incubation of which revealed an accumulation of TASQs in both the cytoplasm and nucleoplasm, therefore testifying for a high bioavailability.[68] Though indirect, it allowed for a wise selection of excitation/emission wavelengths, which opened the way towards colocalization studies: it was used to colocalize nuclear G4 and DNA damage sites, which provided unique insights into the mechanism of action of G4 targeting agents as DNA damage increased upon cell incubation with the G4-ligand PDS, while the G4-destabilizer PhpC reversed G4-mediated DNA damage (*unpublished*).

Finally, the most recent TASQ prototypes, named **MultiTASQ**, **photoMultiTASQ** and **azidoMultiTASQ** (Figure 6A), combined the skills of the previous TASQ generations with an additional level of modularity.[77] Their clickable handle (an alkyne for **MultiTASQ** and

photoMultiTASQ, an azide for **azidoMultiTASQ**) allowed them for being implemented in a series of bioorthogonal investigations: they can indeed be clicked (the copper-catalyzed azide-alkyne cycloaddition (CuAAC)[78-79] for **MultiTASQ** and **photoMultiTASQ**, the strain-promoted azide-alkyne cycloaddition (SPAAC)[80] for **azidoMultiTASQ**) once in interaction with their cellular partners with, for instance, a biotin for affinity capture (*e.g.*, click-seq)[81] or a fluorophore for visualization purposes (*e.g.*, *in situ* click imaging, Figure 6H).[82] The photoactivatable diazirine handle of **photoMultiTASQ** was specifically designed to capture and profile G4-interacting proteins (*i.e.*, the co-binding-mediated protein profiling (CMPP) protocol),[83] which add a proteomics component to the already well-advance genomics use of TASQ. This patented technology[29] thus offers new and wide-ranging opportunities to go increasingly further in the study of cellular G4s at a multi-omics scale.

Outlook

The logic behind the development of the 14 different TASQs described herein was to provide the G4 community with ever smarter and user friendly molecular tools to decipher the biology of DNA and RNA G4s. Our philosophy was to address different but complementary questions regarding G4s with tools form the same family, in order to make these sets of results comparable. We believe this is being achieved, even if TASQs are course not devoid of limitations including their cumbersome synthesis, their moderate G4-affinity, their inability to discriminate between G4s of different nature (DNA, RNA) and topologies, and a possible but not-yet-observed random association with C-rich sequences. Another limitation is the scope of application of TASQs, which remains, for now, limited to cell-based investigations. An extension towards small animal studies could be envisaged but will require to both rethink the design of TASQs (to make them, for instance, detectable *via* whole-body imaging) and address key points (such as their physiological stability, metabolization, drug-induced organ toxicity, etc.). This is an open canvas where much remains to be done and uncovered.

These shortcomings notwithstanding, we believe that these tools have proven efficient and versatile enough for a broad series of *in vitro* investigations to be successful, which address most of the questions relevant today on G4 biology. We also believe that the time is ripe to benefit from this outstanding wealth of knowledge to meet new challenges. Indeed, G4s can boast of being at the very heart of a special attention for 2 decades now. However,

accumulating evidence now shows that other higher-order nucleic acid structures deserves to be granted such special treatment:[84] this includes i-motifs,[73] R-loops,[85] triplex-DNA[86] and DNA junctions,[87] for which ligands and protocols have been yet devised, but not in a finely orchestrated manner (as G4s did), which has somewhat dampened the advance of these investigations. Let us wager that the coming years will deliver fascinating advances in these areas, which will undoubtedly find multiple applications in the field of genetics and genetic diseases.

On a more personal note, the results presented herein provide a strong message that unformal discussions occurring during conferences (and poster sessions) might lead to an entirely new area of research, even if I think that neither Jeff and I would have envisioned at that time that this open discussion would take us from simple supramolecular chemistry considerations to deep, multi-omics investigations.

Acknowledgments

This work would not have been possible without the support of different funding agencies (the CNRS, ANR, ISITE BFC, ERDF, Plan Cancer and European Union) and the contribution of talented students, including Loïc Stefan and Romain Haudecoeur (DOTASQs), Aurélien Laguerre (PyroTASQ and N-TASQ), Pauline Lejault (BioTASQ) and Francesco Rota Sperti (CyTASQs, TriazoTASQs and MultiTASQs); of enthusiastic coworkers, either locally (chiefly, Ibai E. Valverde and Marc Pirrotta) or abroad (chiefly, Sunny Y. Yang and Judy M. Wong (CA), Andrey S. Tsvetkov (USA) and Wenli Zhang (China)); of dedicated collaborators I have the chance to work with on different (more or less G4-free) projects; and of all scientists worldwide who contribute every day to make the G4 field a lively and thrilling research area.

Conflict of interest

The CNRS has licensed BioCyTASQ and MultiTASQs to Merck KGaA for commercialization.

Biography

David Monchaud received his PhD in chemistry 2002 at the University of Geneva (Switzerland) under the supervision of Prof. Jérôme Lacour. After two post-docs in Paris (France), he was appointed as a CNRS researcher in 2005 in the laboratory of Prof. Jean-Marie Lehn (College de

France, Paris) under the supervision of Dr. Marie-Paule Teulade-Fichou, before moving to Institut Curie (Orsay) in 2007 with Dr. Teulade-Fichou. He then joined the Institut de Chimie Moléculaire de l'Université de Bourgogne (ICMUB, Dijon, France) in 2009, where he became CNRS Research Director in 2017, to develop chemical genetics programs on DNA/RNA secondary structures, smart ligands and probes.

References

1. Haudecoeur, R.; Stefan, L.; Denat, F.; Monchaud, D., A Model of Smart G-Quadruplex Ligand. *J. Am. Chem. Soc.* **2013,** *135*, 550-553.
2. Laguerre, A.; Hukezalie, K.; Winckler, P.; Katranji, F.; Chanteloup, G.; Pirrotta, M.; Perrier-Cornet, J.-M.; Wong, J. M.; Monchaud, D., Visualization of RNA-quadruplexes in live cells. *J. Am. Chem. Soc.* **2015,** *137*, 8521-8525.
3. Yang, S. Y.; Lejault, P.; Chevrier, S.; Boidot, R.; Robertson, A. G.; Wong, J. M.; Monchaud, D., Transcriptome-wide identification of transient RNA G-quadruplexes in human cells. *Nat. Commun.* **2018,** *9*, 4730.
4. Mitteaux, J.; Lejault, P.; Wojciechowski, F.; Joubert, A.; Boudon, J.; Desbois, N.; Gros, C. P.; Hudson, R. H. E.; Boulé, J.-B.; Granzhan, A.; Monchaud, D., Identifying G-Quadruplex-DNA-Disrupting Small Molecules. *J. Am. Chem. Soc.* **2021,** *143*, 12567-12577.
5. Davis, J. T., G-quartets 40 years later: From 5 '-GMP to molecular biology and supramolecular chemistry. *Angew. Chem. Int. Ed.* **2004,** *43*, 668-698.
6. Watson, J. D.; Crick, F. H., Molecular structure of nucleic acids. *Nature* **1953,** *171*, 737-738.
7. Hoogsteen, K., The structure of crystals containing a hydrogen-bonded complex of 1-methylthymine and 9-methyladenine. *Acta Crystallogr.* **1959,** *12*, 822-823.
8. Stefan, L.; Monchaud, D., Applications of guanine quartets in nanotechnology and chemical biology. *Nat. Rev. Chem.* **2019,** *3*, 650-668.
9. Wilson, W. D.; Sugiyama, H., First International Meeting on Quadruplex DNA. *ACS Chem. Biol.* **2007,** *2*, 589-594.
10. Kaucher, M. S.; Harrell, W. A.; Davis, J. T., A unimolecular G-quadruplex that functions as a synthetic transmembrane Na+ transporter. *J. Am. Chem. Soc.* **2006,** *128*, 38-39.
11. De Cian, A.; DeLemos, E.; Mergny, J.-L.; Teulade-Fichou, M.-P.; Monchaud, D., Highly efficient G-quadruplex recognition by bisquinolinium compounds. *J. Am. Chem. Soc.* **2007,** *129*, 1856-1857.
12. Nikan, M.; Sherman, J. C., Template-assembled synthetic G-quartets (TASQs). *Angew. Chem. Int. Ed.* **2008,** *47*, 4900-4902.
13. Davis, J. T.; Spada, G. P., Supramolecular architectures generated by self-assembly of guanosine derivatives. *Chem. Soc. Rev.* **2007,** *36*, 296-313.
14. Rhodes, D.; Lipps, H. J., G-quadruplexes and their regulatory roles in biology. *Nucleic Acids Res.* **2015,** *43*, 8627-8637.
15. Crick, F., Central dogma of molecular biology. *Nature* **1970,** *227*, 561.
16. Varshney, D.; Spiegel, J.; Zyner, K.; Tannahill, D.; Balasubramanian, S., The regulation and functions of DNA and RNA G-quadruplexes. *Nat. Rev. Mol. Cell Biol.* **2020,** *21*, 459-474.
17. Lansdorp, P., Telomere Length Regulation. *Frontiers in Oncology* **2022,** *12*, 943622.

18. Chen, L.; Dickerhoff, J.; Sakai, S.; Yang, D., DNA G-Quadruplex in Human Telomeres and Oncogene Promoters: Structures, Functions, and Small Molecule Targeting. *Acc. Chem. Res.* **2022,** *18*, 2628-2646.
19. Duquette, M. L.; Handa, P.; Vincent, J. A.; Taylor, A. F.; Maizels, N., Intracellular transcription of G-rich DNAs induces formation of G-loops, novel structures containing G4 DNA. *Genes Dev.* **2004,** *18*, 1618-1629.
20. Rodriguez, R.; Miller, K. M.; Forment, J. V.; Bradshaw, C. R.; Nikan, M.; Britton, S.; Oelschlaegel, T.; Xhemalce, B.; Balasubramanian, S.; Jackson, S. P., Small-molecule-induced DNA damage identifies alternative DNA structures in human genes. *Nat. Chem. Biol.* **2012,** *8*, 301-310.
21. Di Antonio, M.; Ponjavic, A.; Radzevičius, A.; Ranasinghe, R. T.; Catalano, M.; Zhang, X.; Shen, J.; Needham, L.-M.; Lee, S. F.; Klenerman, D.; Balasubramanian, S., Single-molecule visualization of DNA G-quadruplex formation in live cells. *Nat. Chem.* **2020,** *12*, 832-837.
22. Zell, J.; Rota Sperti, F.; Britton, S.; Monchaud, D., DNA folds threaten genetic stability and can be leveraged for chemotherapy. *RSC Chem. Biol.* **2021,** *2*, 47-76.
23. Neidle, S., Quadruplex Nucleic Acids as Novel Therapeutic Targets. *J. Med. Chem.* **2016,** *59*, 5987-6011.
24. Jackson, S. P.; Bartek, J., The DNA-damage response in human biology and disease. *Nature* **2009,** *461*, 1071-1078.
25. Kosiol, N.; Juranek, S.; Brossart, P.; Heine, A.; Paeschke, K., G-quadruplexes: A promising target for cancer therapy. *Mol. Cancer* **2021,** *20*, 40.
26. Read, M.; Harrison, R. J.; Romagnoli, B.; Tanious, F. A.; Gowan, S. H.; Reszka, A. P.; Wilson, W. D.; Kelland, L. R.; Neidle, S., Structure-based design of selective and potent G quadruplex-mediated telomerase inhibitors. *Proc. Natl. Acad. Sci. U. S. A.* **2001,** *98*, 4844-4849.
27. Rodriguez, R.; Mueller, S.; Yeoman, J. A.; Trentesaux, C.; Riou, J.-F.; Balasubramanian, S., A Novel Small Molecule That Alters Shelterin Integrity and Triggers a DNA-Damage Response at Telomeres. *J. Am. Chem. Soc.* **2008,** *130*, 15758-15758.
28. Olivieri, M.; Cho, T.; Álvarez-Quilón, A.; Li, K.; Schellenberg, M. J.; Zimmermann, M.; Hustedt, N.; Rossi, S. E.; Adam, S.; Melo, H.; Heijink, A. M.; Sastre-Moreno, G.; Moatti, N.; Szilard, R. K.; McEwan, A.; Ling, A. K.; Serrano-Benitez, A.; Ubhi, T.; Feng, S.; Pawling, J.; Delgado-Sainz, I.; Ferguson, M. W.; Dennis, J. W.; Brown, G. W.; Cortés-Ledesma, F.; Williams, R. S.; Martin, A.; Xu, D.; Durocher, D., A Genetic Map of the Response to DNA Damage in Human Cells. *Cell* **2020,** *182*, 481-496.e21.
29. Monchaud, D.; Valverde, I. E.; Lejault, P.; Rota Sperti, F. Biomimetic G-quartet compounds. WO2021198239, Oct 07, 2021, 2021. BioCy: https://www.sigmaaldrich.com/FR/en/product/mm/sct246 - https://www.sigmaaldrich.com/FR/en/product/mm/sct247
30. Stefan, L.; Guedin, A.; Amrane, S.; Smith, N.; Denat, F.; Mergny, J.-L.; Monchaud, D., DOTASQ as a prototype of nature-inspired G-quadruplex ligand. *Chem. Commun.* **2011,** *47*, 4992-4994.
31. Murat, P.; Gennaro, B.; Garcia, J.; Spinelli, N.; Dumy, P.; Defrancq, E., The Use of a Peptidic Scaffold for the Formation of Stable Guanine Tetrads: Control of a H-bonded Pattern in Water. *Chem. Eur. J.* **2011,** *17*, 5791-5795.
32. Stefan, L.; Duret, D.; Spinelli, N.; Defrancq, E.; Monchaud, D., Closer to nature: an ATP-driven bioinspired catalytic oxidation process. *Chem. Commun.* **2013,** *49*, 1500-1502.

33. Bare, G. A. L.; Liu, B.; Sherman, J. C., Synthesis of a Single G-Quartet Platform in Water. *J. Am. Chem. Soc.* **2013,** *135*, 11985-11989.
34. De Rache, A.; Mergny, J.-L., Assessment of selectivity of G-quadruplex ligands via an optimised FRET melting assay. *Biochimie* **2015,** *115*, 194-202.
35. Laguerre, A.; Levillain, M.; Stefan, L.; Haudecoeur, R.; Katranji, F.; Pirrotta, M.; Monchaud, D., Synthetic G-Quartets as Versatile Nanotools for the Luminescent Detection of G-Quadruplexes. *Chimia* **2015,** *69*, 530-536.
36. Stefan, L.; Bertrand, B.; Richard, P.; Le Gendre, P.; Denat, F.; Picquet, M.; Monchaud, D., Assessing the Differential Affinity of Small Molecules for Noncanonical DNA Structures. *ChemBioChem* **2012,** *13*, 1905-1912.
37. Xu, H.-J.; Stefan, L.; Haudecoeur, R.; Sophie, V.; Richard, P.; Denat, F.; Barbe, J.-M.; Gros, C. P.; Monchaud, D., Porphyrin-templated synthetic G-quartet (PorphySQ): a second prototype of G-quartet-based G-quadruplex ligand. *Org. Biomol. Chem.* **2012,** *10*, 5212-5218.
38. Laguerre, A.; Desbois, N.; Stefan, L.; Richard, P.; Gros, C. P.; Monchaud, D., Porphyrin-Based Design of Bioinspired Multitarget Quadruplex Ligands. *ChemMedChem* **2014,** *9*, 2035-2039.
39. Haudecoeur, R.; Stefan, L.; Monchaud, D., Multitasking Water-Soluble Synthetic G-Quartets: From Preferential RNA-Quadruplex Interaction to Biocatalytic Activity. *Chem. Eur. J.* **2013,** *19*, 12739-12747.
40. Gabelica, V., Native Mass Spectrometry and Nucleic Acid G-Quadruplex Biophysics: Advancing Hand in Hand. *Acc. Chem. Res.* **2021,** *54*, 3691-3699.
41. Adrian, M.; Heddi, B.; Phan, A. T., NMR spectroscopy of G-quadruplexes. *Methods* **2012,** *57*, 11-24.
42. Umar, M. I.; Ji, D.; Chan, C.-Y.; Kwok, C. K., G-Quadruplex-Based Fluorescent Turn-On Ligands and Aptamers: From Development to Applications. *Molecules* **2019,** *24*, 2416.
43. Østergaard, M. E.; Hrdlicka, P. J., Pyrene-functionalized oligonucleotides and locked nucleic acids (LNAs): Tools for fundamental research, diagnostics, and nanotechnology. *Chem. Soc. Rev.* **2011,** *40*, 5771-5788.
44. Laguerre, A.; Stefan, L.; Larrouy, M.; Genest, D.; Novotna, J.; Pirrotta, M.; Monchaud, D., A Twice-As-Smart Synthetic G-Quartet: PyroTASQ Is Both a Smart Quadruplex Ligand and a Smart Fluorescent Probe. *J. Am. Chem. Soc.* **2014,** *136*, 12406-12414.
45. Doucet, H.; Hierso, J. C., Palladium-based catalytic systems for the synthesis of conjugated enynes by Sonogashira reactions and related alkynylations. *Angew. Chem. Int. Ed.* **2007,** *46*, 834-871.
46. Gilli, G.; Bellucci, F.; Ferretti, V.; Bertolasi, V., Evidence for resonance-assisted hydrogen bonding from crystal-structure correlations on the enol form of the. beta.-diketone fragment. *J. Am. Chem. Soc.* **1989,** *111*, 1023-1028.
47. Fonseca Guerra, C.; Zijlstra, H.; Paragi, G.; Bickelhaupt, F. M., Telomere structure and stability: covalency in hydrogen bonds, not resonance assistance, causes cooperativity in guanine quartets. *Chem. Eur. J.* **2011,** *17*, 12612-12622.
48. Zhou , J.; Roembke, B. T.; Paragi , G.; Laguerre , A.; Sintim, H. O.; Fonseca Guerra , C.; Monchaud, D., Computational understanding and experimental characterization of twice-as-smart quadruplex ligands as chemical sensors of bacterial nucleotide second messengers. *Sci. Rep.* **2016,** *6*, 33888.

49. Shinamura, S.; Osaka, I.; Miyazaki, E.; Nakao, A.; Yamagishi, M.; Takeya, J.; Takimiya, K., Linear- and Angular-Shaped Naphthodithiophenes: Selective Synthesis, Properties, and Application to Organic Field-Effect Transistors. *J. Am. Chem. Soc.* **2011,** *133*, 5024-5035.
50. Dumas, A.; Luedtke, N. W., Cation-Mediated Energy Transfer in G-Quadruplexes Revealed by an Internal Fluorescent Probe. *J. Am. Chem. Soc.* **2010,** *132*, 18004-18007.
51. Biffi, G.; Tannahill, D.; McCafferty, J.; Balasubramanian, S., Quantitative visualization of DNA G-quadruplex structures in human cells. *Nat. Chem.* **2013,** *5*, 182-186.
52. Demchenko, A. P., The red-edge effects: 30 years of exploration. *Lumin.* **2002,** *17*, 19-42.
53. Berger, O.; Adler-Abramovich, L.; Levy-Sakin, M.; Grunwald, A.; Liebes-Peer, Y.; Bachar, M.; Buzhansky, L.; Mossou, E.; Forsyth, V. T.; Schwartz, T.; Ebenstein, Y.; Frolow, F.; Shimon, L. J. W.; Patolsky, F.; Gazit, E., Light-emitting self-assembled peptide nucleic acids exhibit both stacking interactions and Watson–Crick base pairing. *Nat. Nanotechnol.* **2015,** *10*, 353-360.
54. Amor, S.; Yang, S. Y.; Wong, J. M.; Monchaud, D., Cellular Detection of G-Quadruplexes by Optical Imaging Methods. *Curr. Protoc. Cell Biol.* **2017**, 4.33. 1-4.33. 19.
55. Yang, S. Y.; Amor, S.; Laguerre, A.; Wong, J. M.; Monchaud, D., Real-time and quantitative fluorescent live-cell imaging with quadruplex-specific red-edge probe (G4-REP). *Biochim. Biophys. Acta* **2017,** *1861*, 1312-1320.
56. Yang, S. Y.; Chang, E. Y. C.; Lim, J.; Kwan, H. H.; Monchaud, D.; Yip, S.; Stirling, Peter C.; Wong, J. M. Y., G-quadruplexes mark alternative lengthening of telomeres. *NAR Cancer* **2021,** *3*, zcab031.
57. Moruno-Manchon, J. F.; Lejault, P.; Wang, Y.; McCauley, B.; Honarpisheh, P.; Scheihing, D. A. M.; Singh, S.; Dang, W.; Kim, N.; Urayama, A.; Zhu, L.; Monchaud, D.; McCullough, L. D.; Tsvetkov, A. S., Small-molecule G-quadruplex stabilizers reveal a novel pathway of autophagy regulation in neurons. *eLife* **2020,** *9*, e52283.
58. Lejault, P.; Moruno-Manchon, J. F.; Vemu, S. M.; Honarpisheh, P.; Zhu, L.; Kim, N.; Urayama, A.; Monchaud, D.; McCullough, L. D.; Tsvetkov, A. S., Regulation of autophagy by DNA G-quadruplexes. *Autophagy* **2020,** *16*, 2252-2259.
59. Tabor, N.; Ngwa, C.; Mitteaux, J.; Meyer, M. D.; Moruno-Manchon, J. F.; Zhu, L.; Liu, F.; Monchaud, D.; McCullough, L. D.; Tsvetkov, A. S., Differential responses of neurons, astrocytes, and microglia to G-quadruplex stabilization. *Aging* **2021,** *13*, 15917-15941.
60. Harvey, R. G., Advances in the synthesis of polycyclic aromatic compounds. *Curr. Org. Chem.* **2004,** *8*, 303-323.
61. Laitinen, O. H.; Nordlund, H. R.; Hytönen, V. P.; Kulomaa, M. S., Brave new (strept) avidins in biotechnology. *Trends Biotechnol.* **2007,** *25*, 269-277.
62. Renard, I.; Grandmougin, M.; Roux, A.; Yang, S. Y.; Lejault, P.; Pirrotta, M.; Wong, J. M. Y.; Monchaud, D., Small-molecule affinity capture of DNA/RNA quadruplexes and their identification in vitro and in vivo through the G4RP protocol. *Nucleic Acids Res.* **2019,** *47*, 5502-5510.
63. Lyu, K.; Chow, E. Y.-C.; Mou, X.; Chan, T.-F.; Kwok, Chun K., RNA G-quadruplexes (rG4s): genomics and biological functions. *Nucleic Acids Res.* **2021,** *49*, 5426-5450.
64. Kwok, C. K.; Marsico, G.; Sahakyan, A. B.; Chambers, V. S.; Balasubramanian, S., rG4-seq reveals widespread formation of G-quadruplex structures in the human transcriptome. *Nat. Meth.* **2016,** *13*, 841-844.
65. Guo, J. U.; Bartel, D. P., RNA G-quadruplexes are globally unfolded in eukaryotic cells and depleted in bacteria. *Science* **2016,** *353*, aaf5371.

66. Brosh, R. M.; Matson, S. W., History of DNA Helicases. *Genes* **2020,** *11*, 255.
67. Lejault, P.; Mitteaux, J.; Rota Sperti, F.; Monchaud, D., How to untie G-quadruplex knots and why? *Cell Chem. Biol.* **2021,** *28*, 436-455.
68. Rota Sperti, F.; Charbonnier, T.; Lejault, P.; Zell, J.; Bernhard, C.; Valverde, I. E.; Monchaud, D., Biomimetic, Smart, and Multivalent Ligands for G-Quadruplex Isolation and Bioorthogonal Imaging. *ACS Chem. Biol.* **2021,** *16*, 905-914.
69. Le, D. D.; Di Antonio, M.; Chan, L. K. M.; Balasubramanian, S., G-quadruplex ligands exhibit differential G-tetrad selectivity. *Chem. Commun.* **2015,** *51*, 8048-8050.
70. Feng, Y.; Luo, Z.; Rota Sperti, F.; Valverde, I. E.; Zhang, W.; Monchaud, D., Chemo-versus immuno-precipitation of G-quadruplex-DNA (G4DNA): a direct comparison of the efficiency of the antibody BG4 versus the small-molecule ligands TASQs for G4 affinity capture. *Research Square* **2022**. DOI: 10.21203/rs.3.rs-1717207/v1
71. Feng, Y.; Tao, S.; Zhang, P.; Rota Sperti, F.; Liu, G.; Cheng, X.; Zhang, T.; Yu, H.; Wang, X.-e.; Chen, C.; Monchaud, D.; Zhang, W., Epigenomic features of DNA G-quadruplexes and their roles in regulating rice gene transcription. *Plant Physiol.* **2022,** *188*, 1632-1648.
72. Chambers, V. S.; Marsico, G.; Boutell, J. M.; Di Antonio, M.; Smith, G. P.; Balasubramanian, S., High-throughput sequencing of DNA G-quadruplex structures in the human genome. *Nat. Biotechnol.* **2015,** *33*, 877-881.
73. Abou Assi, H.; Garavís, M.; González, C.; Damha, M. J., i-Motif DNA: structural features and significance to cell biology. *Nucleic Acids Res.* **2018,** *46*, 8038-8056.
74. Ma, X.; Feng, Y.; Yang, Y.; Li, X.; Shi, Y.; Tao, S.; Cheng, X.; Huang, J.; Wang, X.-e.; Chen, C.; Monchaud, D.; Zhang, W., Genome-wide characterization of i-motifs and their potential roles in the stability and evolution of transposable elements in rice. *Nucleic Acids Res.* **2022,** *50*, 3226-3238.
75. Peña Martinez, C. D.; Zeraati, M.; Rouet, R.; Mazigi, O.; Gloss, B.; Chan, C.-L.; Bryan, T. M.; Smith, N. M.; Dinger, M. E.; Kummerfeld, S.; Christ, D., Human genomic DNA is widely interspersed with i-motif structures. *bioRxiv* **2022**, 2022.04.14.488274.
76. Rota Sperti, F.; Dupouy, B.; Mitteaux, J.; Pipier, A.; Pirrotta, M.; Chéron, N.; Valverde, I. E.; Monchaud, D., Click-Chemistry-Based Biomimetic Ligands Efficiently Capture G-Quadruplexes In Vitro and Help Localize Them at DNA Damage Sites in Human Cells. *JACS Au* **2022,** *2*, 1588-1595.
77. Rota Sperti, F.; Mitteaux, J.; Zell, J.; Pipier, A.; Valverde, I. E.; Monchaud, D., The multivalent G-quadruplex (G4)-ligands MultiTASQs allow for versatile click chemistry-based investigations. *bioRxiv* **2022**, 2022.10.28.512542.
78. Tornøe, C. W.; Christensen, C.; Meldal, M., Peptidotriazoles on solid phase:[1, 2, 3]-triazoles by regiospecific copper (I)-catalyzed 1, 3-dipolar cycloadditions of terminal alkynes to azides. *J. Org. Chem.* **2002,** *67*, 3057-3064.
79. Rostovtsev, V. V.; Green, L. G.; Fokin, V. V.; Sharpless, K. B., A Stepwise Huisgen Cycloaddition Process: Copper(I)-Catalyzed Regioselective "Ligation" of Azides and Terminal Alkynes. *Angew. Chem. Int. Ed.* **2002,** *41*, 2596-2599.
80. Agard, N. J.; Prescher, J. A.; Bertozzi, C. R., A Strain-Promoted [3 + 2] Azide−Alkyne Cycloaddition for Covalent Modification of Biomolecules in Living Systems. *J. Am. Chem. Soc.* **2004,** *126*, 15046-15047.
81. Tyler, D. S.; Vappiani, J.; Cañeque, T.; Lam, E. Y.; Ward, A.; Gilan, O.; Chan, Y.-C.; Hienzsch, A.; Rutkowska, A.; Werner, T.; Wagner, A. J.; Lugo, D.; Gregory, R.; Molina, C. R.; Garton, N.; Wellaway, C. R.; Jackson, S.; MacPherson, L.; Figueiredo, M.; Stolzenburg, S.; Bell, C. C.; House, C.; Dawson, S.-J.; Hawkins, E. D.; Drewes, G.; Prinjha, R. K.; Rodriguez, R. l.;

Grandi, P.; Dawson, M. A., Click chemistry enables preclinical evaluation of targeted epigenetic therapies. *Science* **2017,** *356*, 1397-1401.
82. Cañeque, T.; Müller, S.; Rodriguez, R., Visualizing biologically active small molecules in cells using click chemistry. *Nat. Rev. Chem.* **2018,** *2*, 202-215.
83. Zhang, X.; Spiegel, J.; Martínez Cuesta, S.; Adhikari, S.; Balasubramanian, S., Chemical profiling of DNA G-quadruplex-interacting proteins in live cells. *Nat. Chem.* **2021,** *13*, 626-633.
84. Wang, G.; Vasquez, K. M., Dynamic alternative DNA structures in biology and disease. *Nat. Rev. Genet.* **2022**. DOI: 10.1038/s41576-022-00539-9
85. Crossley, M. P.; Bocek, M.; Cimprich, K. A., R-Loops as Cellular Regulators and Genomic Threats. *Mol. Cell* **2019,** *73*, 398-411.
86. Dalla Pozza, M.; Abdullrahman, A.; Cardin, C. J.; Gasser, G.; Hall, J. P., Three's a crowd – stabilisation, structure, and applications of DNA triplexes. *Chem. Sci.* **2022,** *13*, 10193-10215.
87. McQuaid, Kane T.; Pipier, A.; Cardin, Christine J.; Monchaud, D., Interactions of small molecules with DNA junctions. *Nucleic Acids Res.* **2022,** *50*, 12636-12656.